PROCEEDINGS OF ECOS 2023 - THE 36TH INTERNATIONAL CONFERENCE ON
EFFICIENCY, **C**OST, **O**PTIMIZATION, **S**IMULATION AND ENVIRONMENTAL IMPACT OF ENERGY SYSTEMS
25-30 JUNE, 2023, LAS PALMAS DE GRAN CANARIA, SPAIN

A seasonal assessment of a hybrid combined heat and power system with green hydrogen storage in Rio de Janeiro (Brazil) through an energetic, exergetic, exergoeconomic, and environmental analysis

José Eduardo Sanson Portella de Carvalho[a], Romuald Rullière[b], Rémi Revellin[c] and Florian Pradelle[d]

[a] Pontifícia Universidade Católica do Rio de Janeiro, Rio de Janeiro, Brazil, Univ Lyon, INSA Lyon, CNRS, CETHIL, UMR5008, 69621 Villeurbanne, France, zecarvalho07@gmail.com
[b] Univ Lyon, INSA Lyon, CNRS, CETHIL, UMR5008, 69621 Villeurbanne, France, romuald.rulliere@insa-lyon.fr,
[c] Univ Lyon, INSA Lyon, CNRS, CETHIL, UMR5008, 69621 Villeurbanne, France, remi.revellin@insa-lyon.fr,
[d] Pontifícia Universidade Católica do Rio de Janeiro, Rio de Janeiro, Brazil, pradelle@puc-rio.br,

Abstract:

The increasing energy and environmental crises require a shift in worldwide energy management, with the broader use of energy storage, and an increase in the share of renewable energy sources, in particular for electricity generation. Such a process is called energy transition. Thus, low-carbon (or green) hydrogen produced by water electrolysis from renewable electricity is one of the most promising options, since it can be used in fuel cells, with a high-efficiency operation, and without harmful emissions. Thus, this work investigates through a numerical simulation in Matlab, a cogeneration system used to supply electricity and heat demands for an on-grid residence in the city of Rio de Janeiro, Brazil. The original configuration for the hybrid combined heat and power (CHP) system is composed of photovoltaic (PV) panels, which exceeding energy feeds a proton exchange membrane electrolyzer cells (PEMEC) to produce hydrogen that is compressed and then stored. When the PV system is not able to supply the demand, the produced green hydrogen is then blended with natural gas to feed a solid oxide fuel cell (SOFC). Natural gas burner is used as an auxiliary source for heat generation when the SOFC is not operating. The energetic, exergetic, exergoeconomic, and environmental (4E) performances are assessed on a typical day of each season. Results indicate that the system can stably operate with moderate energy and exergy efficiencies for both the SOFC and PEMEC. Blending hydrogen with natural gas also allow a reduction of CHP specific emissions. The high availability of unused heat also strongly suggests the addition of an absorption chiller to increase the global system efficiency.

Keywords:

Proton exchange membrane electrolyzer cells (PEMEC); Solid oxide fuel cell (SOFC); Hydrogen compression, Renewable energy; 4E analysis; Numerical study.

Nomenclature

A	Area, m²	f_k	Exergoeconomic factor
$\dot{C}$	Cost rate, $/s	F	Faraday constant. C/mol
c	Unit cost, $/GJ	h	Specific enthalpy, kJ/kg
e	Specific entropy, kJ/(kg.K)	I	Electric current, A
$\dot{E}$	Exergy Rate, W	I_L	Light current, A

https://doi.org/10.52202/069564-0126

I_0	Reversible saturation current, A
J	Current density, A/m²
k	Boltzmann constant, m².kg/(s².K)
K	Equilibrium constant
LHV	Lower heating value, MJ/kg
$\dot{m}$	Mass flow rate, kg/s
N	Number of cells
$\dot{n}$	Molar flow rate, mol/s
P	Pressure, kPa
$\dot{P}$	Electric Power, W
q	Electron charge, C
$\dot{Q}$	Heat exchange rate, W
r	Recirculation factor
R	Resistance, Ω
R_u	Universal Gas Constant, J/(K.mol)
T	Temperature, K
U	Utilization factor
V	Voltage, V
V_{act}	Activation voltage, V
V_{ohm}	Ohmic voltage, V
V_{conc}	Concentration voltage, V
$\dot{W}$	Power, kW
X	Molar fraction
$\dot{Z}$	Levelized cost, $/s

Greek symbols

η	Efficiency
v	Stoichiometry coefficient

Subscript

bu	Burner
c	Compressor
cell	Cell
con	Consumption
d	Destruction
dem	Demand
ele	Electric
f	Fuel
gen	Generation
hxc	Heat exchanger's cold stream
hxh	Heat exchanger's hot stream
i	Inlet
j	Surrounding
p	Pump
PV	Photovoltaic
q	Heat
rh	Recoverable heat
ther	Thermal
W	Work

1. Introduction

The demand for low environmental impact and renewable power sources is steadily increasing. Thus, there is a growing installed capacity of power generation from renewable resources, particularly wind turbines (WT) and photovoltaic panels (PV), which are widely adopted. During the day, PV systems convert incident solar radiation into electricity, while WT systems harness the wind's favorable conditions to rotate the blades and produce electricity. Combining these two systems offers a viable solution for enhancing the reliability of power generation, even though they increased the complexity of the grid management. Since both PV and WT are intermittent energy sources, it is crucial to incorporate a storage system to enhance overall efficiency and provide the demand during the whole day. Hydrogen emerges as a promising alternative due to its high energy density in weight basis, minimal energy loss, well-established technology, on-site provision capability, and reliability comparable to conventional fuels such as coal, nuclear, and natural gas [1]. Among the most promising methods for hydrogen production is water electrolysis, while the current predominant approach involves fossil fuel conversion (mainly by steam reforming of natural gas). The resulting hydrogen, known as green hydrogen, has emerged as a potential solution for future decarbonization efforts [2].

Additionally, the interest in efficient technology that offers a wide range of useful energy products and services, such as polygeneration, is increasing significantly. Polygeneration system involves an integrated process that produces multiple energy outputs from a single energy source. Among the possible technology, the fuel cells are energy conversion devices that play a key role in generating electricity through an electrochemical reaction between a fuel (mainly hydrogen) and an oxidant. This direct conversion of chemical energy into electricity eliminates the need for a combustion process. Significant attention has been directed towards Solid Oxide Fuel Cells (SOFC) due to their superior efficiency, long-term stability, and low emissions during operation. Operating at high temperatures (ranging from 650 to 1000 °C), SOFCs enable the reforming process to occur within the cell itself. This allows the SOFCs to be fed with natural gas and remove the need to reduce the carbon monoxide content of the reformate, making them an excellent choice for cogeneration, trigeneration, and multigeneration applications [3]. Numerous studies have examined the feasibility and thermal performance of SOFCs within complex systems. In trigeneration systems, where electricity generation is the primary function of SOFCs, previous studies have observed the utilization of heat exchangers to recover exhaust gas heat, along with refrigeration systems (typically with absorption chillers) to provide cold demand [4–7]. Parameters such as current density [4,7–16] and SOFC operating temperature [4,8–10,14,17] have been extensively investigated in the literature. Furthermore, some studies have conducted exergoeconomic evaluations of the system [9–16,18], while a few have undertaken environmental analyses [10,12,14,18].

https://doi.org/10.52202/069564-0126

Many studies have focused on the utilization of electrolysis to produce hydrogen. Among the electrolyser technologies, the polymer electrolyte membrane electrolyser (PEMEC) is the most widely used in the recent projects and the literature showed that it is adaptable for integration with different systems. The advantage of PEMEC is its rapid response, making it suitable for transient conditions, while producing high-purity hydrogen at relatively low temperatures (around 50 to 90°C) [19]. Literature reviews have demonstrated the integration of PEMEC in systems that harness renewable resources [20–23]. Similarly to SOFCs, the process parameters investigated for the optimization of the PEMEC operation include current density [20,22,24] and operating temperature [21–23].

Even though the renewables reached 44.7% of the energy mix, with sugarcane biomass and hydroelectricity accounting for the largest shares at 16.4% and 11% respectively, a recent study examining the Brazilian energy matrix highlighted a decline in the contribution of renewable energy sources due to water scarcity and an increased reliance on thermoelectric plants. Despite solar and wind power having a smaller share at 2.5% and 10.6% respectively, they experienced significant year-on-year increases of 55.9% and 26.7%. In terms of energy consumption, the residential sector accounted for approximately 10.9% of Brazil's energy use, while the transport and industrial sectors combined represented a consumption of 64.5%. The installed capacity for energy generation demonstrated an overall increase of 3.9%, with solar and wind power leading the growth at 40.9% and 21.2% respectively. In the realm of micro/mini distributed generation, solar power witnessed a remarkable 88.3% increase compared to the previous year [25].

Regarding hydrogen in the country, the Energy National Plan 2050 (PNE 2050) recognizes hydrogen as a disruptive technology and a crucial element for the decarbonization of the energy matrix. The plan highlights the diverse uses and applications of hydrogen and provides recommendations for energy policies to promote the development of the chain values, including production, transport, storage, and consumption, in the country. Key guidelines include assessing opportunities for blue hydrogen production from natural gas and green hydrogen production using renewable energy sources, called “rainbow” approach. Additionally, the plan emphasizes exploring the production of hydrogen from biofuels (bioethanol, biomethane and glycerine) and using existing infrastructure for the transition, such as incorporating hydrogen into the natural gas pipeline network [26,27]. The integration of hydrogen into natural gas has the potential to enhance the role of natural gas, abundant in the Pre-salt fields, as a low-carbon transition fuel while simultaneously scaling up hydrogen production, particularly from renewable sources [2].

As demonstrated earlier, there are a limited number of studies in the literature that conduct a energetic, exergetic, economic, and environmental (4E) analysis of a cogeneration system. Furthermore, no research has been found that specifically examines the impact of seasonality on a hybrid system that integrates renewable power generation and consumption using both PEMEC and SOFC technologies. Although the share of solar power is not so expressive into the Brazilian energy matrix, its growth is noticeable, along with an increasing interest for hydrogen production. In light of these factors, this study aims to evaluate a hybrid combined heat and power (CHP) system with green hydrogen storage in Rio de Janeiro, Brazil. The evaluation focuses on a typical day from each season for a residential building. An hourly-based analysis is performed, considering the electricity and heat demand of a standard building. The study specifically assesses the energetic, exergetic, exergoeconomic, and environmental aspects of the system through a comprehensive 4E analysis. To achieve this, various parameters are examined, including system efficiencies, carbon dioxide emission rates, cost per unit of exergy, and the exergoeconomic factor. The aim is to provide a thorough understanding of the system's performance and quantify its impact in terms of energy, exergy, economics, and the environment.

2. System description

The representation of the hydrogen storage system is shown in Figure 1. A renewable module comprised of a set of photovoltaic panels in series and parallel is responsible for extracting energy from the sun and supplying an electric demand. If there is a surplus of power in this process, the system operates in what is called the generation mode, otherwise, if there is a shortage, it works in the consumption mode. In the first mode, the surplus energy from the renewable module is used to supply power for an electrolyzer which together with water, generates green hydrogen and oxygen. The hydrogen is compressed into a pressurized tank, to be later used in any case of need. To supply the heat demand, a natural gas burner is triggered. For the other mode of operation, hydrogen from the tank is withdrawn and goes through the expansion valve to be mixed with natural gas and then preheated in a heat exchange before entering the reformer. Water is also preheated before entering the reformer, and after the reforming process, the products and a preheated air feed the solid oxide fuel cell for the electrochemical process. The generated electricity passes through the inverter priorly to being supplied to the final user. The depleted fuel and air from the SOFC go into an afterburner for complete combustion of carbon monoxide, methane, and hydrogen, and the exhaust gases are used for preheating the mixture (hydrogen-natural gas), water, and air. Then, the exhaust gases pass by a heat exchanger to supply the user’s heat demand. This module consists of a hot tank, a pump, and a pair of heat exchangers (exhaust gas and hot water). The tank is assumed to be sufficiently large to be considered isothermal. Finally, the hot exhaust gases from the afterburner are cooled down to ambient temperature.

https://doi.org/10.52202/069564-0126

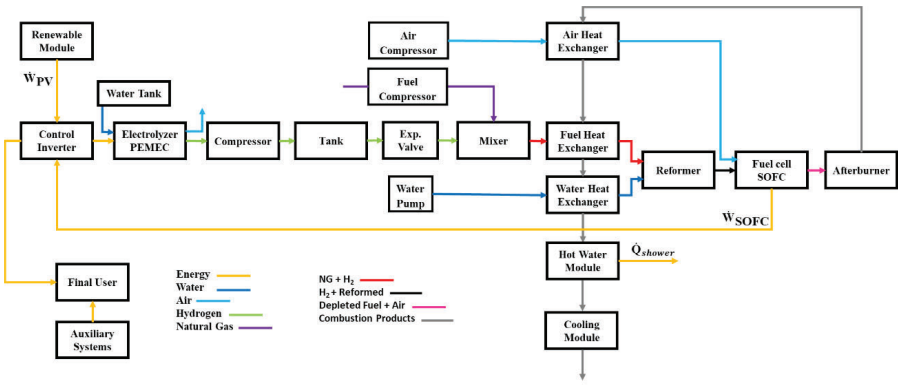

Figure 1. Schematic representation of the hydrogen storage system.

For this system's simulation, a steady-state condition under thermodynamic equilibrium is assumed for each investigated instant of time. All components are assumed to be well insulated, thus no heat loss from equipment to the environment is considered. Compressors and pumps operate with isentropic efficiency equal to 0.85, and the heat exchangers have a constant efficiency during operation of 0.9 with no pressure drop. The mixing chamber, reformer, natural gas burner, and afterburner operate at constant pressure, and their outlet species composition and temperature are calculated using energy and mass balance. The inverter has a constant efficiency of 0.95. All gases are treated as an ideal gas, dry air composition is considered 21% O_2 and 79% N_2, and natural gas is considered as pure methane. The compressed hydrogen is stored at 300 bar and ambient temperature. The properties of all fluids are based on the Peng-Robinson equation of state, having as reference state for gases temperature at 298.15 K and 0.101325 MPa.

3. Modeling

This section focuses on displaying the main equations for the system's components. The extensive equating can be found in Appendix A, and the parameters for the system in Appendix B [28].

3.1. Renewable module: photovoltaic panels (PV)

This module consists of a combination of photovoltaic panels producing electric power at an optimized current and voltage [29,30]. This system's performance presents a non-linear current-voltage curve, Eq. (1):

$$I=I_L-I_0\left(\exp\left(\frac{q(V+IR)}{\gamma k T_{cell}}\right)-1\right) \quad (1)$$

The panels are set to work at maximum power output adjusting both voltage and current to reach such conditions

3.2. Proton exchange membrane electrolyzer (PEMEC)

A proton exchange membrane electrolyzer is used to generate hydrogen using the surplus energy from the renewable module. The rate of the produced hydrogen is defined by a function of the current density and number of electrolyzers considered, Eq. (2) [5,31]:

$$\dot{n}_{H_2}=\eta_f\frac{NI}{2F} \quad (2)$$

The actual voltage of the electrolyzer is defined by a function of its reversible voltage and losses, Eq. (3) [11,32]:

$$V=V_0+V_{act}+V_{ohm} \quad (3)$$

3.3. Solid oxide fuel cell (SOFC)

The amount of hydrogen entering the anode in the electric reaction of the solid oxide fuel cell is also described by the current density operation, Eq. (4) [33]:

$$\dot{n}_{H_2}=\frac{JA\,(1-r+rU_f)n}{2\,F\,U_f} \quad (4)$$

The process for calculating the inlet on the cathode side and the outlet of both the anode and cathode are described in Colpan et al. [33].

The actual voltage of the solid oxide fuel cell is described in Eq. (5) [4,11,32]:

$$V=V_0-V_{act}-V_{ohm}-V_{conc} \quad (5)$$

3.4. Reformer

Fuel reforming reactions allow the conversion of fuel (natural gas blended with hydrogen into another one through a catalytic reaction, from a less active one into one more active. Thermodynamic equilibrium is assumed for the considered chemical reactions and described by the general equilibrium constant, Eq. (6):

$$K_{e,i} = \prod_i x_i^{v_i} \left(\frac{P}{P_0}\right)^{\sum_i v_i} \quad (6)$$

3.5. 4E analysis

Such analysis comprehends assessing the components, and the whole system, as control volumes through an energetic, exergetic, exergoeconomic, and environmental point of view. To do so, mass, energy exergy, and cost balances are considered, Eqs. (7-11) [34]:

$$\sum \dot{m}_o = \sum \dot{m}_i \quad (7)$$

$$\dot{Q} - \dot{W} = \sum_o \dot{m}_o h_o - \sum_i \dot{m}_i h_i \quad (8)$$

$$\dot{E}_D = \sum_j \left(1 - \frac{T_0}{T_j}\right) \dot{Q}_j - \dot{W} + \sum_i \dot{m}_i e_i - \sum_o \dot{m}_o e_o \quad (9)$$

$$\sum \dot{C}_i + \dot{C}_q + \dot{Z} = \sum \dot{C}_o + \dot{C}_w \quad (10)$$

$$\dot{C} = c\dot{E} \quad (11)$$

Table B.1 displays the capital equation of each component [28].

The environmental analysis considers the amount of carbon dioxide emitted during the system operation, through the combustion of natural gas and the depleted fuel of the solid oxide fuel cell, and its mitigation due to the addition of hydrogen in the blend with natural gas.

The electric and thermal efficiencies of the system are used to assess the system's performance. They are described as follows in Eqs. (12-15):

$$\eta_{ele,gen} = \frac{\dot{P}_{dem} + \dot{m}_{H_2} LHV_{H_2} + \dot{W}_{c,H_2}}{\dot{W}_{PV} + \dot{W}_{c,H_2}} \quad (12)$$

$$\eta_{ele.con} = \frac{\dot{P}_{dem} + \dot{W}_{c,all} + \dot{W}_{p,all}}{\dot{W}_{PV} + \dot{W}_{Grid} + \dot{m}_{H_2} LHV_{H_2} + \dot{W}_{c,all} + \dot{W}_{p,all}} \quad (13)$$

$$\eta_{ther,gen} = \frac{\dot{Q}_{dem}}{\dot{Q}_{bu}} \quad (14)$$

$$\eta_{ther,con} = \frac{\dot{Q}_{hxc,all} + \dot{Q}_{dem}}{\dot{Q}_{hxh,all} + \dot{Q}_{ts} + \dot{Q}_{rh} + \dot{Q}_{bu}} \quad (15)$$

For the exergoeconomic evaluation, the exergoeconomic factor, Eqs. (16-17), and unit cost of the SOFC and PEMEC are considered.

$$f_k = \frac{\dot{Z}}{\dot{Z} + \dot{C}_d} \quad (16)$$

$$\dot{C}_d = c_f \dot{E}_d \quad (17)$$

The unit cost expresses the average cost at which each unit of fuel is supplied to a component or the average cost at which exergy unit was supplied to a product. The exergoeconomy factor expresses the contribution of the capital cost to the sum of capital cost and exergy destruction, providing a measurement of the component cost-effectiveness.

4. Numerical solution

The solution of the system relies on the hourly interaction between the solar radiation and the electric demand of the building through one day for each season of the year. Figure 2 displays the flowchart of the steps taken for solving the system. The parameters considered in this work concerning the building, photovoltaic panels, SOFC, and PEMEC dimensioning are shown in Appendix B [28].

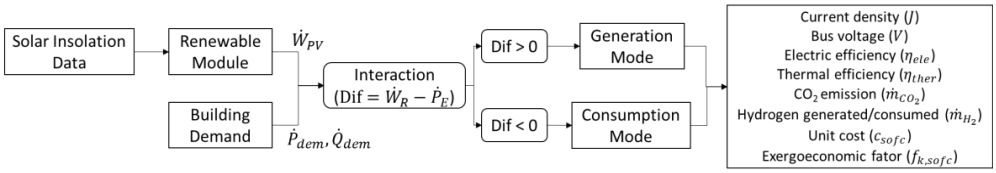

Figure 2: System's solution flowchart.

https://doi.org/10.52202/069564-0126

4.1. Electric power and heat demands

The electricity demand of a typical residential building from Rio de Janeiro is evaluated using the typical profile curve of residential consumption together with the historical average value for each month [35]. It is possible to observe a higher consumption in summer due to the hot temperatures in the country, as a higher amount of air conditioners are working. Spring and Autumn have similar electric demands. Water heating for showers is the only source of heat demand in the Rio de Janeiro context [36]. Both demands are displayed in Figure 3.

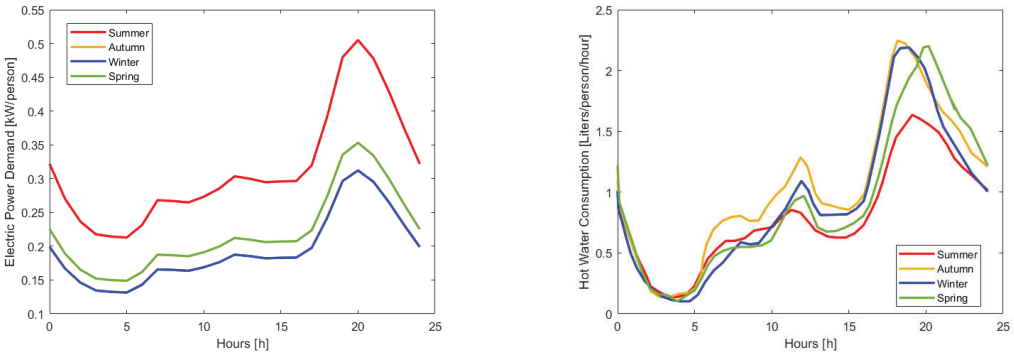

(a) (b)

Figure. 3. a) Electric power demand per person. b) Hot water profile of a typical Brazilian residential building.

4.2. Solar Radiation and interaction

As previously said, the difference between the electric power coming from the renewable module and the electricity demands dictates the functioning of the system. Figure 4 presents both the solar radiation for a characteristic day of each season in Rio de Janeiro and the aforementioned difference for the Summer. The area above the zero line (orange) corresponds to the generation mode, while the area under the line (blue) corresponds to the consumption mode.

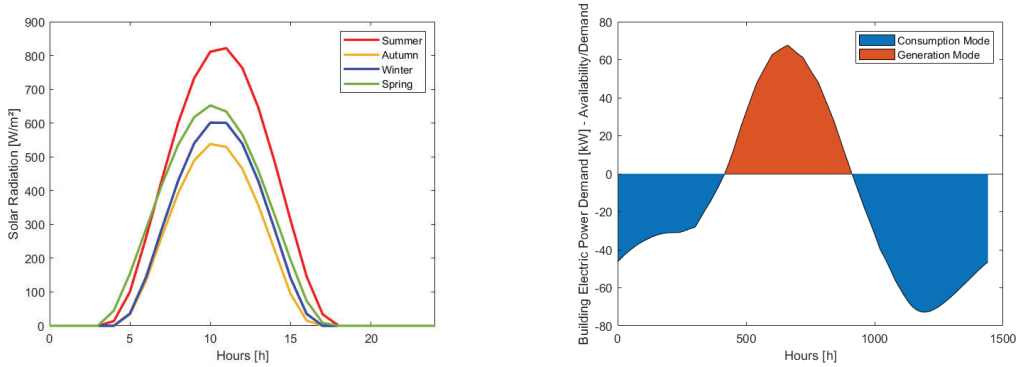

(a) (b)

Figure. 4. a) Solar radiation in Rio de Janeiro for the characteristic day of each season. b) Data regarding availability and demand of electric power.

4.3. Generation path

The stacks of PEMEC work accordingly to the amount of available power, turning on and off to the necessary number of stacks for the operation. Both current density and the stack's bus voltage are adjusted in this process so the system can operate at the highest efficiency. Having the final condition set, the amount of green hydrogen produced and the electrolyzer's parameter can be calculated. The variables considered in this study for the PEMEC are displayed in Table B.4.

4.4. Consumption path

When the electric power from the renewable module is not enough to meet the user's demand, the stacks of solid oxide fuel cells are required to generate the missing power. Similarly to the generation path, the stacks can be turned on and off, as a function of the missing electric power, and the stack's current density and bus voltage are adjusted so the system can operate at the highest efficiency. The rate of hydrogen consumption is

calculated in function of the SOFC module's electric power output, and with that, it is possible to infer the amount of natural gas withdrawn from the grid, hydrogen from the tank, and steam necessary for the reforming process using a mass balance on the SOFC reformer. The parameters of the SOFC are shown in Table B.5. After the process in the SOFC, the depleted air and fuel passes through an afterburner for a complete combustion reaction. The hot combustion products are used to heat the hydrogen-natural gas blend and water entering the reformer, and the air entering the cell.

5. Results

5.1. Validation

Both PEMEC and SOFC were modeled according to data taken from the literature [37,38], and results are shown in Appendix B [28]. Tables B.6 and B.7 display a comparison with the values for voltages of each component, and it can be seen a good agreement between this study and the corresponding experimental data.

5.2. Season analysis

To assess the seasonality effect on the system, a characteristic day of each season was chosen, being in the middle of February, May, August, and November to represent Summer, Autumn, Winter, and Spring respectively. Thus, in each case, the current density and bus voltage of both SOFC and PEMEC are controlled and adjusted to supply and use the exact amount of electric power and operate at the highest efficiency. The adjustment for the current density is seen in Figure 5.

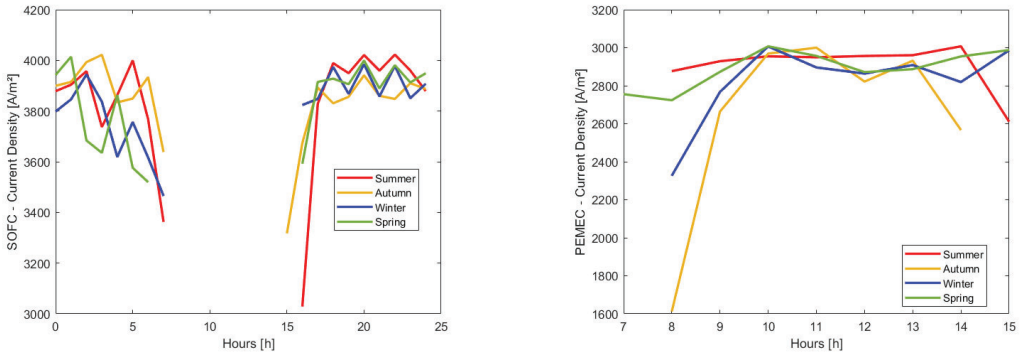

(a) (b)

Figure. 5. Current density. a) SOFC. b) PEMEC.

Figure 5 illustrates a distinct behavior in controlling the current density of both components. In the case of the SOFC, a decrease in current density corresponds to an expected increase in bus voltage, whereas for the PEMEC, the bus voltage decreases as the current density decreases. This phenomenon can be attributed to the nature of the actual voltage definitions for both components, as described in Sections 3.2 and 3.3. Specifically, a lower current density for the SOFC leads to higher voltages, while the opposite is observed for the PEMEC. The values of current density are determined by the electric power to be supplied or utilized by the components, where lower electric power results in lower current density.Hydrogen consumption and generation during operation are also a consequence of the electric power, as shown in Figure 6.

https://doi.org/10.52202/069564-0126

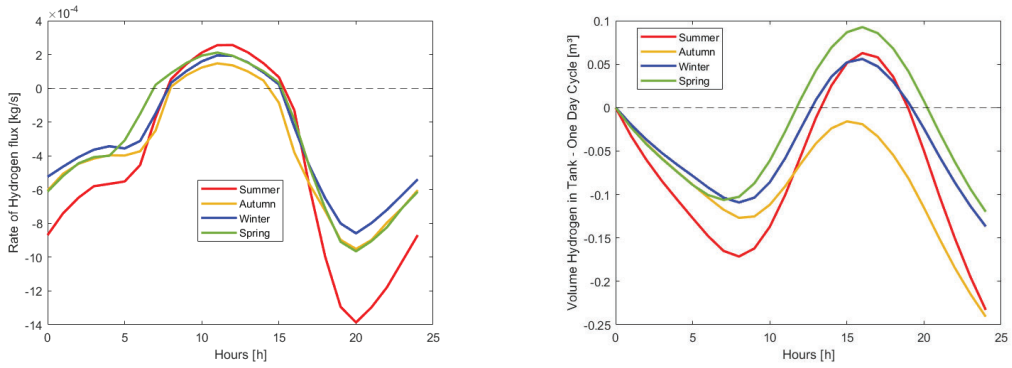

(a) (b)

Figure. 6. Rate of hydrogen generated and consumed. b) Hydrogen volume variation inside the tank.

In Figure 6a, when the curve has a negative or positive value, it corresponds to hydrogen consumption or generation, respectively. During the summer, higher generation and consumption are observed, as expected due to increased electric power demand and solar insolation, as shown in Figures 3a and 4a. Figure 6b illustrates the amount of hydrogen that entered or left the tank after a full day of operation. The greatest variations are observed in the summer, reflecting higher consumption and solar insolation. Consequently, there is a greater fluctuation in the hydrogen level within the tank. These results indicate that, under the given conditions, more hydrogen is consumed than generated each day during every season. By integrating the curve in Figure 6a, the total amount consumed can be calculated, confirming that summer has the highest consumption, followed by autumn, spring, and winter. These findings enable the design of storage tank autonomy and the development of a strategy to control hydrogen availability, such as limiting generation to specific times or blending hydrogen with natural gas in lower quantities.

Figure 7 helps to understand the behavior of the system to supply electricity, and consequently the heat demands.

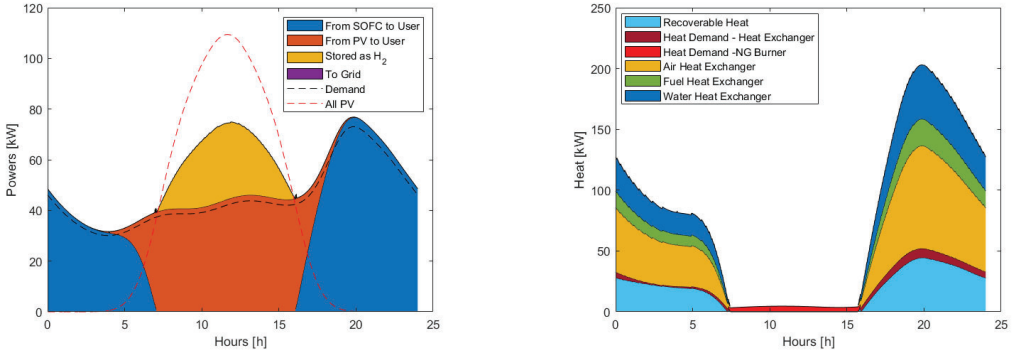

(a) (b)

Figure. 7. Month of February. a) Electric power supply. b) Heat supply.

When there is no energy being generated by the renewable module, the solid oxide fuel cell becomes responsible for supplying all the electric power (blue area). Its contribution gradually decreases as the photovoltaic system begins to supply a portion of the demand (orange area), until a point is reached where the photovoltaic system supplies all the energy, resulting in an excess. When there is an excess, the energy is converted into hydrogen (yellow area) and stored in a tank. Figure 7a shows the losses associated with hydrogen generation by comparing the total power supplied by the photovoltaic system (red dashed line) with the yellow area. It is important to note that both the solid oxide fuel cell and the photovoltaic system deliver more power than the electric demand to account for losses in the inverter. The heat response (Figure 7b) is directly proportional to the number of fuel cells in operation and exhibits a similar behavior to the electric power shown in Figure 7a. The exhaust gases from the afterburner can preheat the fuel, air, and water used in the process and fulfil the building's heat demand. The curve labelled "Recoverable Heat" represents the cooling of the exhaust gases to ambient conditions and could be utilized for a trigeneration process, such as powering an absorption chiller to meet the cooling demand.

The system's electric and thermal efficiencies are assessed in Figure 8.

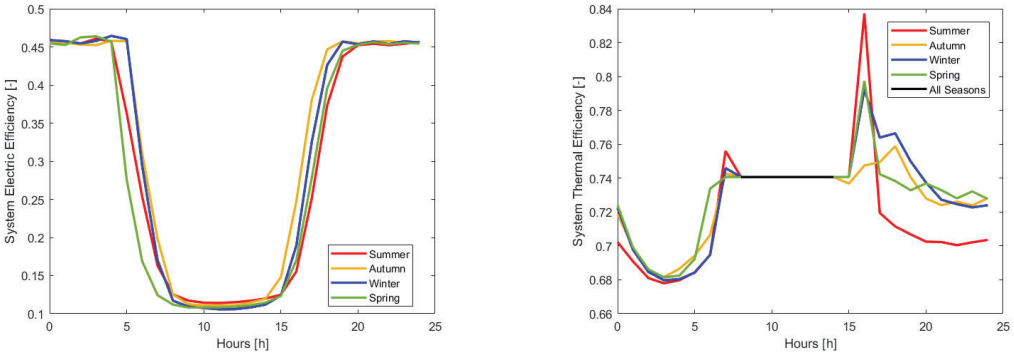

(a) (b)

Figure. 8. a) System's electric efficiency. b) System's thermal efficiency.

Figure 8a demonstrates that the system maintains a steady efficiency when only the SOFC operates to supply the electric power. This behavior is attributed to the control method, which adjusts both the current density and bus voltage to meet the electric power demand. As the photovoltaic panels begin to contribute to the electric power supply, the overall efficiency of the system starts to decrease due to the panels' lower efficiency. Additionally, in the energy surplus region, there is a further decrease in efficiency caused by losses in hydrogen generation through the PEMEC. By examining Figure 8b, it can be observed that the thermal efficiency of the system remains constant during the generation mode, with a natural gas burner efficiency of 0.74. However, during the consumption mode, the variations among seasons primarily stem from different hot water profiles and the number of operational cells.

Figure 9 displays the results for both the rate of CO_2 emitted and the influence of hydrogen in the blend during summer.

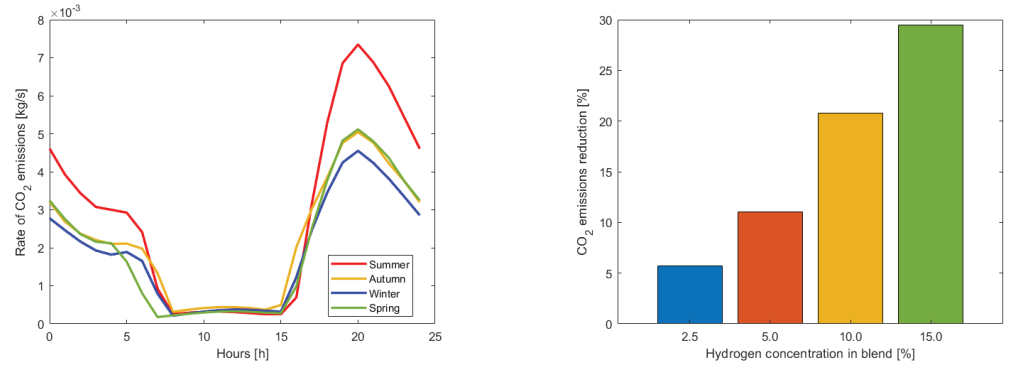

(a) (b)

Figure. 9. a) Rate of CO_2 emission. b) Carbon dioxide emission reduction due to hydrogen addition to the blend.

The carbon dioxide emission, Figure 9a, is described as a function of the electricity demand of the consumption mode, and as a function of heat demand of the generation mode. A higher amount of functioning fuel cells would imply a higher amount of hydrogen being withdrawn from the tank and natural gas from the grid. Consequently, after the whole process, higher emissions would be seen. It is expected to have a higher emission during the Summer, as the electric demand from the building is also higher. In the generation mode, the amount of emissions is dictated by the heat demand which is supplied by the natural gas burner. Figure 9b displays the influence of adding hydrogen to the blend with natural gas. A higher participation of hydrogen would reduce the emissions of carbon dioxide due to a lesser amount of CO_2 after the reforming process, and consequently after the electrochemical reaction in the SOFC. The addition of 15% of hydrogen, on a mass basis, to the blend would reduce up to 29% of these emissions.

Figure 10 shows the unit cost for both SOFC and PEMEC.

https://doi.org/10.52202/069564-0126

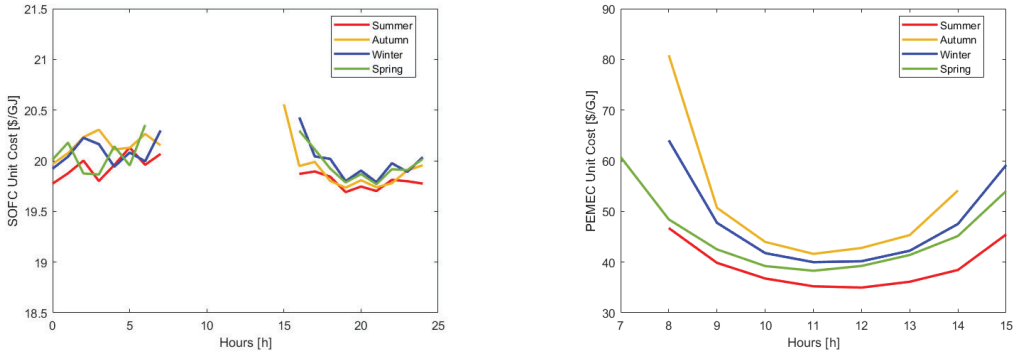

(a) (b)

Figure. 10. Unit cost. a) SOFC. b) PEMEC.

The unit cost of the SOFC shows only minor variations based on seasonality and the time of day. The capital cost of the SOFC is determined by the number of active cells, which is in turn influenced by the user's electric power requirements. Consequently, the relatively stable unit cost arises from the consistent operational efficiency of the system, where the current density is adjusted to meet the electric demand. On the other hand, the unit cost of operation for the PEMEC is greatly impacted by the excess electric power supplied by the PV system. During midday, when solar radiation reaches its peak, the unit cost of operation is lower due to increased hydrogen generation, despite the higher capital cost associated with the PEMECs.

Figure 11 displays the exergoeconomic factor for both components.

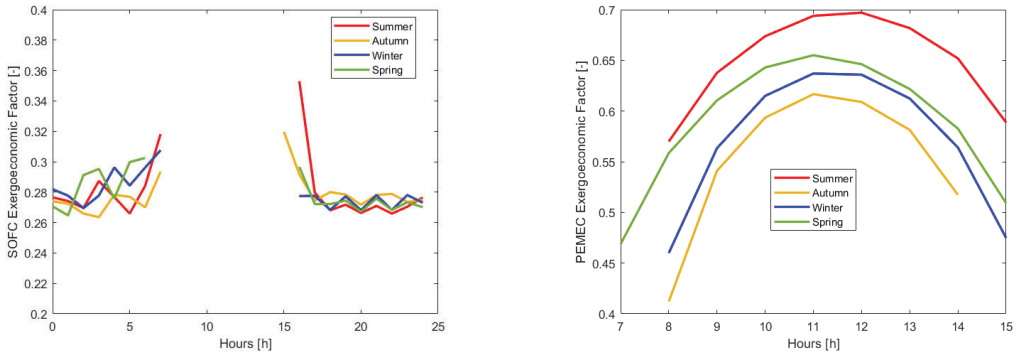

(a) (b)

Figure. 11. Exergoeconomic factor. (a) SOFC. (b) PEMEC.

The behavior of the exergoeconomic factor is similar to the unit cost. Regarding the SOFC, its value is constant for most of the operation, which fluctuations are a result of the current density adjustments. For the PEMEC, the exergoeconomic factor is highly influenced by the supplied electric power, due to the higher values at midday and due to the seasonality, where the summer has a higher radiation compared to the other seasons. A low value of the exergoeconomic factor indicates potential cost savings for the system by reducing exergy destruction, which can be achieved by improving component efficiency, even if it entails increased capital investment. Conversely, a high value of the factor suggests the possibility of reducing the investment cost of the component at the expense of its exergetic efficiency.

6. Conclusion

A hybrid combined CHP system using green hydrogen storage is evaluated in the city of Rio de Janeiro, Brazil. The system is assessed through a 4E standpoint while supplying both electric power and the heat demand of a typical building. The system is mainly composed of a photovoltaic system, a proton exchange membrane electrolyzer, and a solid oxide fuel cell. The system can perform at the rated electricity demand at maximum and stable efficiency while supplying all the heat necessary for its running and hot shower. The amount of hydrogen produced and consumed is estimated and it was seen that during summer, due to a higher solar insulation and electric demand, the variations inside the tank are higher when compared with any other season. Pollutant emissions are strictly related to the number of operating fuel cells, as they would require a higher

amount of fuel, and the addition of hydrogen would reduce the number of such emissions, as less natural gas would be burnt. Recalling the exergoeconomic, it has been shown that seasonality has little effect on the solid oxide fuel cell parameters, while the proton exchange membrane is highly affected by solar radiation. Finally, the system showed the possibility of introducing a cooling system utilizing the recoverable heat in an absorption chiller.

The system seems to be a good option to diversify the use of renewable resources in Brazil, which has hydropower as the main source. With the right design of the tank, the system would be able to sustain both the electricity and heat demand of a typical residential building. In the future, it is desired to analyze the system's functioning during a whole year, compare the results found with demands and weather conditions of other countries, and optimize the system to find the best functioning condition. Additionally, a comparison with other energy storage systems, such as compressed air (CAES), would allow a better understanding of the feasibility of these systems to substitute the ongoing ones.

References

[1] Khalilnejad A, Sundararajan A, Sarwat AI. Optimal design of hybrid wind/photovoltaic electrolyzer for maximum hydrogen production using imperialist competitive algorithm. J Mod Power Syst Clean Energy 2018;6:40–9. https://doi.org/10.1007/s40565-017-0293-0.

[2] IRENA. Hydrogen: A renewable energy perspective. International Renewable Energy Agency; 2019.

[3] Mehr AS, Lanzini A, Santarelli M, Rosen MA. Polygeneration systems based on high temperature fuel cell (MCFC and SOFC) technology: System design, fuel types, modeling and analysis approaches. Energy 2021;228:120613. https://doi.org/10.1016/j.energy.2021.120613.

[4] Chitsaz A, Hosseinpour J, Assadi M. Effect of recycling on the thermodynamic and thermoeconomic performances of SOFC based on trigeneration systems; A comparative study. Energy 2017;124:613–24. https://doi.org/10.1016/j.energy.2017.02.019.

[5] Ranjbar F, Chitsaz A, Mahmoudi SMS, Khalilarya S, Rosen MA. Energy and exergy assessments of a novel trigeneration system based on a solid oxide fuel cell. Energy Conversion and Management 2014;87:318–27. https://doi.org/10.1016/j.enconman.2014.07.014.

[6] Sadeghi M, Chitsaz A, Mahmoudi SMS, Rosen MA. Thermoeconomic optimization using an evolutionary algorithm of a trigeneration system driven by a solid oxide fuel cell. Energy 2015;89:191–204. https://doi.org/10.1016/j.energy.2015.07.067.

[7] Tian M, Yu Z, Zhao H, Yin J. Thermodynamic analysis of an integrated solid oxide fuel cell, Organic Rankine Cycle and absorption chiller trigeneration system with CO2 capture. Energy Conversion and Management 2018;171:350–60. https://doi.org/10.1016/j.enconman.2018.05.108.

[8] Ahmadi S, Ghaebi H, Shokri A. A comprehensive thermodynamic analysis of a novel CHP system based on SOFC and APC cycles. Energy 2019;186:115899. https://doi.org/10.1016/j.energy.2019.115899.

[9] Sadat SMS, Mirabdolah Lavasani A, Ghaebi H. Economic and thermodynamic evaluation of a new solid oxide fuel cell based polygeneration system. Energy 2019;175:515–33. https://doi.org/10.1016/j.energy.2019.03.093.

[10] Hosseinpour J, Chitsaz A, Liu L, Gao Y. Simulation of eco-friendly and affordable energy production via solid oxide fuel cell integrated with biomass gasification plant using various gasification agents. Renewable Energy 2020;145:757–71. https://doi.org/10.1016/j.renene.2019.06.033.

[11] Chitgar N, Moghimi M. Design and evaluation of a novel multi-generation system based on SOFC-GT for electricity, fresh water and hydrogen production. Energy 2020;197:117162. https://doi.org/10.1016/j.energy.2020.117162.

[12] Wu Z, Zhu P, Yao J, Zhang S, Ren J, Yang F, et al. Combined biomass gasification, SOFC, IC engine, and waste heat recovery system for power and heat generation: Energy, exergy, exergoeconomic, environmental (4E) evaluations. Applied Energy 2020;279:115794. https://doi.org/10.1016/j.apenergy.2020.115794.

[13] Habibollahzade A, Gholamian E, Behzadi A. Multi-objective optimization and comparative performance analysis of hybrid biomass-based solid oxide fuel cell/solid oxide electrolyzer cell/gas turbine using different gasification agents. Applied Energy 2019;233–234:985–1002. https://doi.org/10.1016/j.apenergy.2018.10.075.

[14] Xu Y, Luo X, Tu Z. 4E analysis of a SOFC-CCHP system with a LiBr absorption chiller. Energy Reports 2022;8:5284–95. https://doi.org/10.1016/j.egyr.2022.03.202.

[15] Chitsaz A, Mehr AS, Mahmoudi SMS. Exergoeconomic analysis of a trigeneration system driven by a solid oxide fuel cell. Energy Conversion and Management 2015;106:921–31. https://doi.org/10.1016/j.enconman.2015.10.009.

[16] Khani L, Mahmoudi SMS, Chitsaz A, Rosen MA. Energy and exergoeconomic evaluation of a new power/cooling cogeneration system based on a solid oxide fuel cell. Energy 2016;94:64–77. https://doi.org/10.1016/j.energy.2015.11.001.

https://doi.org/10.52202/069564-0126

[17] Wang H, Yu Z, Wang D, Li G, Xu G. Energy, exergetic and economic analysis and multi-objective optimization of atmospheric and pressurized SOFC based trigeneration systems. Energy Conversion and Management 2021;239:114183. https://doi.org/10.1016/j.enconman.2021.114183.
[18] Ghorbani Sh, Khoshgoftar-Manesh MH, Nourpour M, Blanco-Marigorta AM. Exergoeconomic and exergoenvironmental analyses of an integrated SOFC-GT-ORC hybrid system. Energy 2020;206:118151. https://doi.org/10.1016/j.energy.2020.118151.
[19] Ozturk M, Dincer I. A comprehensive review on power-to-gas with hydrogen options for cleaner applications. International Journal of Hydrogen Energy 2021;46:31511–22. https://doi.org/10.1016/j.ijhydene.2021.07.066.
[20] Nafchi FM, Baniasadi E, Afshari E, Javani N. Performance assessment of a solar hydrogen and electricity production plant using high temperature PEM electrolyzer and energy storage. International Journal of Hydrogen Energy 2018;43:5820–31. https://doi.org/10.1016/j.ijhydene.2017.09.058.
[21] Zheng N, Duan L, Wang X, Lu Z, Zhang H. Thermodynamic performance analysis of a novel PEMEC-SOFC-based poly-generation system integrated mechanical compression and thermal energy storage. Energy Conversion and Management 2022;265:115770. https://doi.org/10.1016/j.enconman.2022.115770.
[22] Zhang X, Zeng R, Du T, He Y, Tian H, Mu K, et al. Conventional and energy level based exergoeconomic analysis of biomass and natural gas fired polygeneration system integrated with ground source heat pump and PEM electrolyzer. Energy Conversion and Management 2019;195:313–27. https://doi.org/10.1016/j.enconman.2019.05.017.
[23] Zhang F, Wang B, Gong Z, Zhang X, Qin Z, Jiao K. Development of photovoltaic-electrolyzer-fuel cell system for hydrogen production and power generation. Energy 2023;263:125566. https://doi.org/10.1016/j.energy.2022.125566.
[24] Chitsaz A, Haghghi MA, Hosseinpour J. Thermodynamic and exergoeconomic analyses of a proton exchange membrane fuel cell (PEMFC) system and the feasibility evaluation of integrating with a proton exchange membrane electrolyzer (PEME). Energy Conversion and Management 2019;186:487–99. https://doi.org/10.1016/j.enconman.2019.03.004.
[25] Ministério de Minas e Energia, Empresa de Pesquisa Energética. BEN - Relatório Sínteses 2022 2022.
[26] Ministério de Minas e Energia, Empresa de Pesquisa Energética. Bases para a Consolidação da Estratégia Brasileira do Hidrogênio 2021.
[27] Ministério de Minas e Energia, Empresa de Pesquisa Energética. Programa Nacional do Hidrogenio 2021.
[28] Carvalho JESP, Rullière R, Revellin R, Pradelle FAY. Supplementary data for ECOS 23 2023. https://www.researchgate.net/publication/369503049_Supplementary_Data_-_ECOS23_f804.
[29] Chenni R, Makhlouf M, Kerbache T, Bouzid A. A detailed modeling method for photovoltaic cells. Energy 2007;32:1724–30. https://doi.org/10.1016/j.energy.2006.12.006.
[30] Hosseini M, Dincer I, Rosen MA. Hybrid solar–fuel cell combined heat and power systems for residential applications: Energy and exergy analyses. Journal of Power Sources 2013;221:372–80. https://doi.org/10.1016/j.jpowsour.2012.08.047.
[31] Sánchez M, Amores E, Rodríguez L, Clemente-Jul C. Semi-empirical model and experimental validation for the performance evaluation of a 15 kW alkaline water electrolyzer. International Journal of Hydrogen Energy 2018;43:20332–45. https://doi.org/10.1016/j.ijhydene.2018.09.029.
[32] Gholamian E, Hanafizadeh P, Habibollahzade A, Ahmadi P. Evolutionary based multi-criteria optimization of an integrated energy system with SOFC, gas turbine, and hydrogen production via electrolysis. International Journal of Hydrogen Energy 2018;43:16201–14. https://doi.org/10.1016/j.ijhydene.2018.06.130.
[33] Colpan C, Dincer I, Hamdullahpur F. Thermodynamic modeling of direct internal reforming solid oxide fuel cells operating with syngas. International Journal of Hydrogen Energy 2007;32:787–95. https://doi.org/10.1016/j.ijhydene.2006.10.059.
[34] Bejan A, Tsatsaronis G, Moran M. Thermal Design & Optimization. First. John Wiley & Sons Ltd; 1996.
[35] Empresa de Pesquisa Energética. Metodologia: projeção de curva de carga horária 2020.
[36] Sborz J, Cominato C, Kalbusch A, Henning E. Hourly and daily domestic hot water consumption in social housing dwellings: An analysis in apartment buildings in Southern Brazil. Solar Energy 2022;232:459–70. https://doi.org/10.1016/j.solener.2021.12.067.
[37] Tao G, Virkar A. Intermediate temperature solid oxide fuel cell (IT-SOFC) research and development activities at MSRI. Nineteenth Annual ACERC&ICES Conference, Utah 2005.
[38] Ni M, Leung MKH, Leung DYC. Energy and exergy analysis of hydrogen production by a proton exchange membrane (PEM) electrolyzer plant. Energy Conversion and Management 2008;49:2748–56. https://doi.org/10.1016/j.enconman.2008.03.018.